ISSN 1068-1620, Russian Journal of Bioorganic Chemistry, 2021, Vol. 47, No. 3, pp. 777–783. © Pleiades Publishing, Ltd., 2021.

Quantum Chemical Calculations on Two Compounds of Proquazone and Proquazone Type Calcites as a Calcium Sensing Receptor (CaSR) Inhibitory Profiles

Ahmed Hassen Shntaif[a, 1], Zahraa M. Rashi[b], Zaid H. Al-Sawaff[c, d], and Fatma Kandemirli[e]

[a] *Chemical department, collge of science for woman, Babylon University, Babylon, Iraq*

[b] *Electronic technical department, Babylon institute, Al-furat Al-awsat Technical University, Najaf, Iraq*

[c] *Materials Science and Engineering, Faculty of Engineering and Architecture, Kastamonu University, Kastamonu, 3700 Turkey*

[d] *Medical Instrumentation Technology, Technical Engineering College, Northern Technical University, Mosul, Iraq*

[e] *Biomedical Engineering Department, Faculty of Engineering and Architecture, Kastamonu University, Kastamonu, 3700 Turkey*

Received May 25, 2020; revised June 10, 2020; accepted June 13, 2020

Abstract—A quantum chemical study was done on two compounds of proquazone and proquazone type calcilytics (6-methoxy-1-(propan-2-yl)-4-[4-(propan-2-yl)phenyl]-1,2 dihydroquinazolin-2-one), and (1-{[3-(2-hydroxyethoxy)phenyl]methyl}-6-(prop-2-yn-1-yloxy)-5-[3-(propan-2-yl)phenyl]-1,2-dihydroquinazolin-2-ol), as a calcium-sensing receptor. The study was done in gas phase using DFT/B3LYP method was considered to calculate the energetic behavior and the quantum chemical descriptors such as the energy gap between HOMO and LUMO, the total energy for various orbital transitions, chemical hardness, softness, electrophilicity index, electro-negativity. Besides, a theoretical study was done on the compounds, in order to study and examine the effect of changing the temperature of the molecule which was from (200 to 1000 K) on thermodynamics properties (enthalpy, entropy, heat capacity, and correlation properties). From the results obtained, there was a noticeable difference between the two compounds regarding the chemical parameters, where the first compound seems to be more stable than the second compound.

Keywords: proquazone, proquazone calcilytics, NBO analysis, DFT, thermodynamics, calcium-sensing receptor

DOI: 10.1134/S106816202103016X

INTRODUCTION

Osteoporosis disease is characterized by the case of low bone mass and microarchitectural deterioration of tissue of the bone which leads to bone fragility and increased the risk of fractures [1]. Most of the therapies used for the treatment of osteoporosis disease prevent bone resorption and stop any further bone loss. However, as many osteoporosis patients have already lost an essential amount of the bone at the time of diagnosis, there is a need for an agent that stimulates the new bone formation [2].

At the present time, the commercially available anabolic therapy used for osteoporosis is the PTH (parathyroid hormone) or PTH fragments such as Forteo (teriparatide, the 1–34 fragment of PTH), whom causes a notable increase in the bone mass and reduces vertebral fracture risks.3 However, this peptide is given by injections.

Proquazone (an analgesic) [3] (Fig. 1), was chosen from a huge number of quinazolinone derivatives showing anti-inflammatory activities, Lead optimization led to compounds such as **1** and **2** that showed IC_{50} values in the nanomolar range in the in vitro receptor examination, and also showed the suitable PK- and PTH-release properties as demonstrated in vivo experiments in animals (short Tmax, sharp PTH plasma peak) [4].

In a comparison with established non-steroidal anti-inflammatory drugs, proquazone has two interesting and importing properties: it has an unconventional chemical structure [5] and is non-acidic [6].

The Density functional theory DFT became a regular tool for the first principles of quantum chemical calculations on the electronic structure, and the properties of many molecular systems where no other first-principles methods can achieve similar accuracy at the same low cost especially in the principles [7], DFT replaces the usual (ab ignition) wavefunctions, which

[1] Corresponding author: e-mail: ahmed_79sh@yahoo.com.

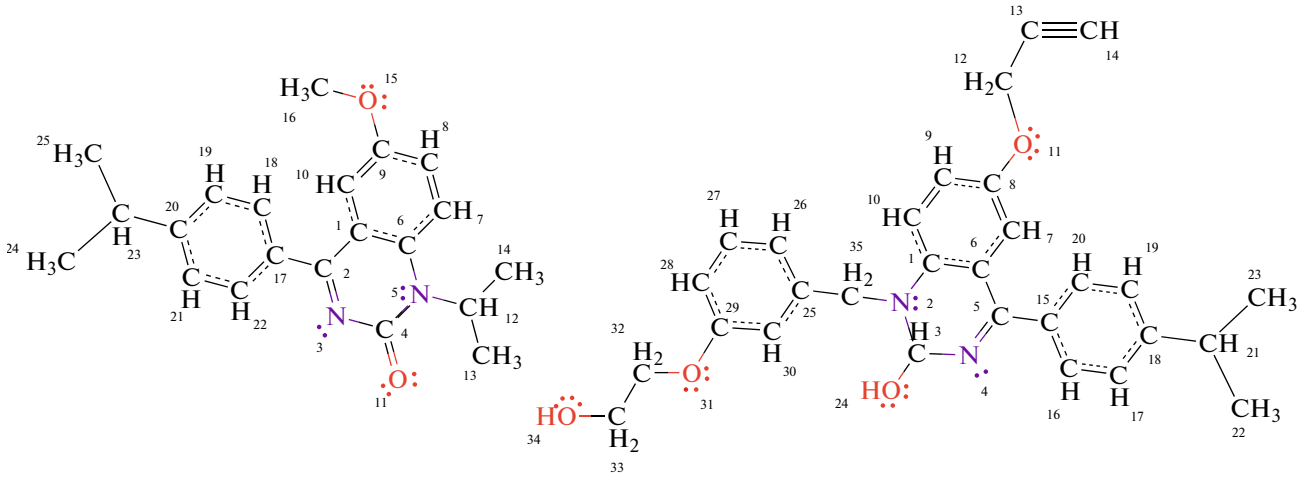

Fig. 1. Proquazone and proquazone type calcilytics.

depend on spatial variables by the electron density which depends only on three spatial variables as a means to reach for a solution to the Schrodinger's equation.

With the exact exchange-correlation functional, DFT can take into full account of all complex effects were unlikely the exact exchange-correlation functional is unknown which making it so essential to follow more and more accurate and reliable approximate functionals [8].

There are almost three categories of density functional methods, first method: Local density approximation (LDA), which assumes that the density of the molecule is uniform throughout the molecule, and is typically not a very popular method. The second method is the gradient corrected (GC) methods look to account for the non-uniformity of the electron density. The last category is the hybrid methods, which attempt to incorporate some of the more useful features from ab initio methods (specifically Hartree-Fock methods) with some of the improvements of DFT mathematics. Hybrid methods, such as B3LYP, tend to be the most generally used methods for computational chemistry practitioners [9].

Computational Method

A three-dimensional analysis was performed to estimate the effect of substitution groups in para, meta, and ortho positions, to produce new derivatives compounds which consider as an ionic monomer and dimer contrast agent, respectively [10]. The geometries of these molecules (6-methoxy-1-(propane-2-yl)-4-[4-(propane-2-yl)phenyl]-1,2-dihydroquinazolin-2-one), and (1-{[3-(2-hydroxyethyl)phenyl]methyl}-6-(prop-2-yn-1-yloxy)-5-[3-(propane-2-yl)phenyl]-1,2-dihydroquinazolin-2-ol) were fully optimized in gas phase by using (Lee-Yang-Parr correlation functional (B3LYP)), and (gradient corrected DFT) with "Becke's three-parameter hybrid exchange functional", and with the B3LYP/6-311G(d,p) basis set.

The High Occupied Molecular Orbitals (HOMO) and Low Unoccupied Molecular Orbital (LUMO) energies and molecular properties related to EHOMO and ELUMO including the hardness (η), softness (s), electronegativity (χ), chemical potential (μ), electrophilicity index (ω), nucleofugality (ΔE_n) and electrofugality (ΔE_n) were calculated, in addition, the change of temperature was investigated to see the final results of heat on the compounds. These parameters were calculated by using the following information [11–13]: The hardness is half of the energy gap between HOMO and LUMO that:

$$\eta \cong \frac{1}{2}(\varepsilon_{HOMO} - \varepsilon_{LUMO}) \cong \frac{1}{2}(I - A). \quad (1)$$

Where A and I are the electron affinity and the ionization potential of the compounds.

The softness can be calculated from hardness that Hard Soft Acid Bas (HSAB) principle is:

$$S = \frac{1}{2\eta}. \quad (2)$$

Electronegativity can be calculated from E_{HOMO} and E_{LUMO} using the following equation:

$$\chi = -\frac{1}{2}(E_{HOMO} + E_{LUMO}). \quad (3)$$

From electronegativity, chemical potential can estimated that $\mu = -\chi$

$$\mu = \frac{1}{2}(E_{HOMO} + E_{LUMO}). \quad (4)$$

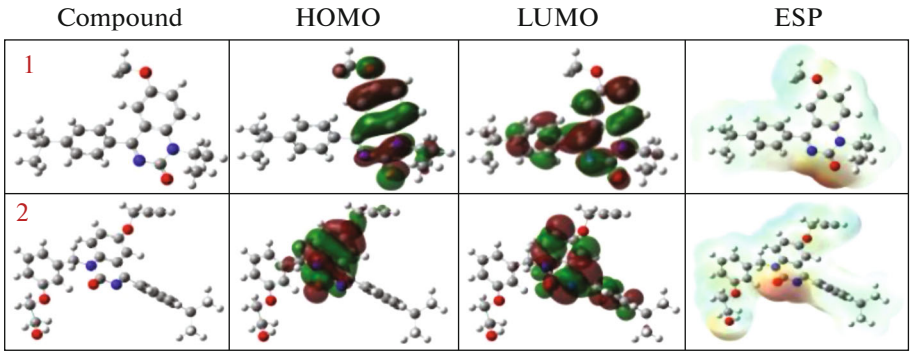

Fig. 2. Optimized structure, HOMO, LUMO, and electron density (ESP) for compound **1** and compound **2**.

Electrophilicity index (ω) and nucleofugality (ΔE_n) and electrofugality (ΔE_e) can be taken from the chemical potential μ, and hardness η by the following equations respectively [14, 15].

$$\text{Nucleofugality } \Delta E_n = (\mu + \eta)2/2\eta, \quad (5)$$

$$\text{Electrophilicity index } \omega = \frac{\mu^2}{2\eta}, \quad (6)$$

$$\text{Electrofugality } \Delta E_e = \frac{(\mu - \eta)^2}{2\eta}. \quad (7)$$

The quantum chemical calculations were performed by employing the density functional theory with Becke3–Lee–Yang–Parr (B3LYP) levels and 6-311G(d,p) basis set by applying it to "Gaussian 09W" program packages [16], and the visual images of the structure, where these properties spectroscopically and electronically, along with the molecular optimization were accomplished by (GaussView 5) software package [17].

RESULTS AND DISCUSSIONS

HOMO/LUMO Analysis

Optimized structure, the highest occupied molecular orbital (HOMO), the lowest unoccupied molecular orbital (LUMO), and electron density of compound **1** and compound **2** in gas phase calculated at DFT/B3LYP level with 6-311G(d,p) basis set are given in Fig. 2. LUMO was mainly localized on benzene and phenyl rings for the studied two compounds, on the other hand, HOMO was mainly localized in the benzene ring.

The potential increases in the order of red < orange < yellow < green < blue [18]. The result is given in the mapped (ESP) have been plotted for the title molecules in the 6-311G basis set using the computer software gauss view. According to red regions are generally localized on the benzene ring in the molecules studied.

The energy gap (ΔE) between the highest occupied molecular orbital (HOMO) and the lowest unoccupied molecular orbital (LUMO) considered as a particularly interesting property for the molecules under study.

The chemical activity of the molecules is related to the energy gap where Table 1 shows the quantum chemical parameters such as E_{HOMO}, E_{LUMO}, polarizability, hardness, softness, chemical potential, and electrophilicity index for compound **1** and compound **2**, using B3LYP/6-311G(d,p) in the gas phase.

Table 1, shows the energies of HOMO which have negative values and they decreased by substitution when B3LYP is used. For instance, the energies of HOMO in the first compound were –5.796 eV. This value decreased in the second compound because of the substitution to became –6.19 eV which was affected by the presence of the benzene ring, likewise, the LUMO energies have negative values and they decreased by substitution for example, in the same method B3LYP, the energy of the first compound was –2.028 eV and decreased to –2.136 eV for the second compound. This note was illustrated in Fig. 3. On the

Table 1. Some quantum chemical parameters

Compound	E_{HOMO}	E_{LUMO}	X (electro negativity)	Hardness	S (softness)	μ (chemical potential)	ω (electrophilicity index)	ΔE_n	ΔE_e
1	–5.796	–2.028	3.912	1.884	0.265	–3.912	4.061	1.091	8.915
2	–6.119	–2.136	4.127	1.992	0.251	–4.127	4.276	1.145	9.399

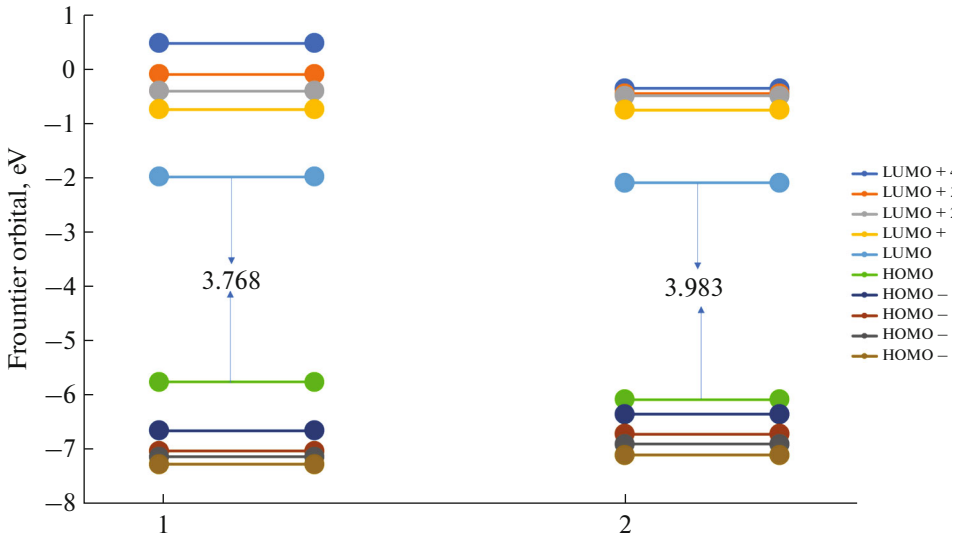

Fig. 3. Energy gap between HOMO and LUMO for the two compounds.

other hand, the change in energy gaps (ΔE) values of the compounds in the gas phase indicated that the energy gaps increased by substitution. As it appears, when tittle compounds in the gas phase were optimized by using B3LYP, the energy gap of the first compound was 3.768 eV and that value increased to become 3.983 eV in the case of the second compound due to the substitution. Also, we can note that the hardness which directly proportional to the energy gap increased from 1.884 eV for the first compound to 1.992 eV for the second compound.

The chemical potential (μ) of the compounds decreased from −3.912 eV for the first compound to −4.127 eV for the second compound. Electrophilicity index (ω), nucleofugality (ΔE_n), and electrofugality (ΔE_e) of the compounds increased by substitution. For example, the optimization of compounds using B3LYP indicate that the electrophilicity index (ω) for the first compound was 4.061 eV, it recorded 4.267 eV for the second compound. Likewise, electrofugality (ΔE_e) and nucleofugality (ΔE_n) were recorded increasing by substitution. Nucleofugality (ΔE_n) was 1.09 eV for the first compound and it was recorded 1.145 eV for the second compound and for electrofugality (ΔE_e) it recorded increasing from 8.915 eV for the first compound to 9.399 eV for the second compound.

NBO Analysis

The NBO analysis is already proved to be an effective tool for chemical interpretation of hyper conjugative interaction and electron density transfer from the filled lone pair electron [19]. The natural charges on atoms and the second-order perturbation energies $E^{(2)}$ (donor–acceptor) of **1**–**6** compounds calculated at B3LYP level with 6-311G(d,p) basis sets were given in Tables 2, 3: 2nd order perturbation theory analysis of the matrix in NBO basis in first and second compounds.

The NBO analysis is already proved to be an effective tool for chemical interpretation of hyper conjuga-

Table 2. Second order perturbation theory analysis of Fock matrix in NBO basis for the two compounds

	Donor (*i*)	ED(*i*)I	Acceptor (*j*)	Type	ED(*j*)I		E^2, kcal/mol	$\varepsilon_j - \varepsilon_i$b, a.u	$F_{i,j}$, a.u
Prog. 1	LP1N2	1.61496	O(1)–C(9)	π*	537	0.34014	46.05	0.28	0.103
	LP1N2	1.61496	C(5)–C(6)	π*	548	0.44830	41.85	0.28	0.098
Prog. 2	LP(1)N2	1.61862	O(1)–C(8)	π*	721	0.32998	46.93	0.29	0.105
	LP(1)N2	1.61862	C(4)–C(5)	π*	729	0.45011	43.51	0.28	0.100

Table 3. Natural Orbital Occupancy (pz)

C1	Position	1	2	3	4	5	6	Ring charge
	Atom	C(8)	N(3)	C(6)	C(5)	C(4)	N(2)	
	Occupancy	0.85255	1.06887	0.98156	1.58346	0.82225	1.22726	0.536
C2	Position	1	2	3	4	5	6	
	Atom	C(7)	C(6)	C(5)	N(2)	C(9)	N(3)	
	Occupancy	1.06287	0.89682	1.08681	1.42957	1.01741	1.31477	0.808

tive interaction and electron density transfer from the filled lone pair electron [20]. The natural charges on atoms and the second-order perturbation energies $E^{(2)}$ (donor–acceptor) of the two compounds calculated at B3LYP level with 6-311G(d,p) basis sets are given in Table 2.

The stabilization energy, E(2), associated with electron delocalization between each donor NBO (i) and the acceptor NBO (j) is found by the following formula. As [20]:

$$E^2 = q_i \frac{(F_{i,j})^2}{\varepsilon_j - \varepsilon_i}, \quad (8)$$

where, q_i is the donor orbital occupancy, ε_i and ε_j are diagonal elements (orbital energies) and $F(i, j)$ is the off-diagonal NBO Fock matrix element [20, 21]. A quantitative standard of the force of interaction between an electron donor and acceptor is provided by the stabilization energy, $E^{(2)}$. The larger $E^{(2)}$ indicates a stronger interaction between the electron donor orbital (i) and the receptor orbital j that is, it means that the tendency to provide an electron to (j) and the degree of electron delocalization are higher [22].

The study of the Natural Bonding Orbitals [NBOs] is illustrated in Tables 2 and 3. The study indicated that the interaction of energy linked to the resonance in the molecule for the electron-donating from lone pair LP 1N2 to π* (O(1)–C(9)) shows the stabilization energy of 46.05 kJ and LP 1N2 to π* (C(6)–C(5)) shows stabilization energy of 41.85 kcal/mole in the first compound. These values increased by substitution in the second compound. LP 1N2 to π* (O(1)–C(8)) shows stabilization energy of 46.93 kcal/mole and LP1N2 to π* (C(4)–C(5)) shows stabilization energy of 43.51 kcal/mole which indicated that these values are affected by the benzene ring in this the second compound. The optimization output of Natural Orbital Occupancy of the mean ring of the two compounds indicated that the charge of the ring is positive and it increased by the substitution from 0.536 eV for the first compound to 0.808 eV.

Thermodynamic Properties

The full energy amount of the molecule can be shown through the total amount of the translation, rotational, electronic energies, and vibrational show where the less amount of energy has been calculated (SCF energy) was agreed with the optimized construction of the molecule [23].

Zero-point vibrational energy is the lowest acceptable amount of energy at the quantum mechanical system, and the desired amount of heat used to make the temperature of any substance higher than the natural amount for one grade is "the capacity of heat" where The quantitative measurement of randomness in any system can be described as the entropy [23].

By using B3LYP/6-311G(d,p) basis set, the parameters of the ordinary statistical thermodynamic properties, like enthalpy (H), heat capacity (C), and entropy (S), for the proquazone and proquazone type calcite were calculated from the theoretical coordination of the frequencies at the range of temperature 200–1000 K in a scale factor of 0.96 [24], as a standard range, furthermore (Fig. 4). Following the equipartition theorem, the translational energy, rotational energy, and molecular vibrational intensities increase with increasing temperature, as a result, the thermodynamic functions increase with increasing temperature ranging from 200 to 1000 K as shown in tables [25]. The linking equations between heat capacity, enthalpy, entropy, and temperature values changing were done by linear and quadratic formulas and the matching suitable factors (R^2) for these thermodynamic properties as for (**1**) and (**2**) compounds, respectively, so by using these equations, without any further computational procedures, was clearly concluded that the characteristics of these compound at any change in any point of temperature, the thermodynamical parameters are linearly dependent on the temperature value [26]. The figures below illustrate the thermodynamic properties change due to the temperature changes with the correlation values for all compounds.

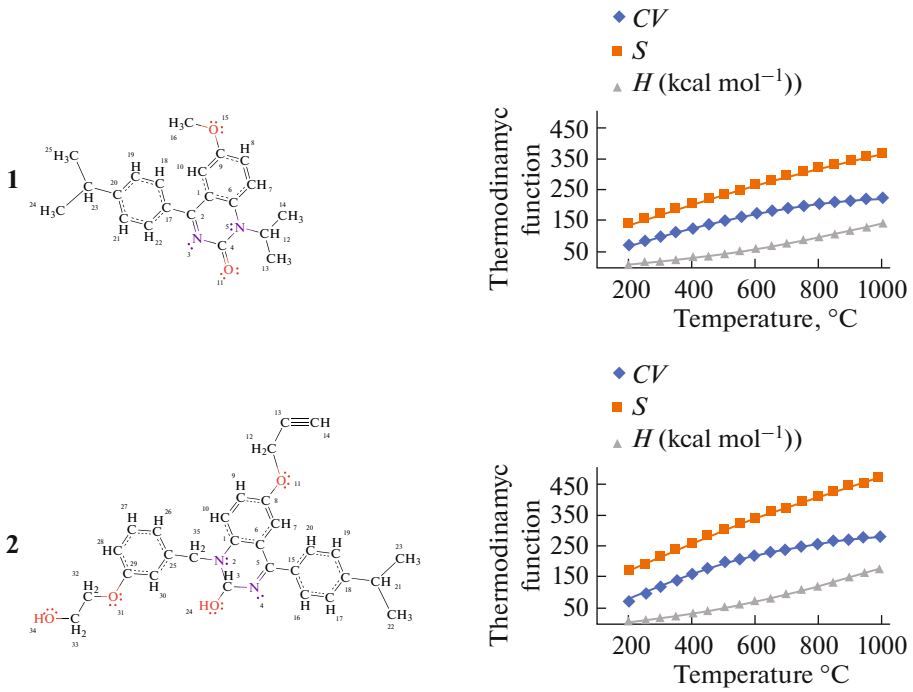

Fig. 4. Clculated thermodynamic parameters for compounds **1** (top) and **2** (bottom).

The correlation equations of the two compounds are as follows

	$S\,(R^2) = 1$	$CV\,(R^2) = 0.9998$	$H\,(R^2) = 0.9998$
1	$y = -8\text{E-}05T^2 + 0.3767T + 62.935$	$y = -0.0002T^2 + 0.3795T - 2.8725$	$y = 9\text{E-}05T^2 + 0.0519T - 7.4566$
2	$y = -0.0001T^2 + 0.509T + 80.955$	$y = -0.0002T^2 + 0.5112T - 3.0709$	$y = 0.0001T^2 + 0.0735T - 10.458$

CONCLUSION

Calculations indicated that the energy gaps values of HOMO vs LUMO in the two compounds were different and were affected by the presence of the benzene ring in the case of the second compound, these changes led to modifications in the other chemical calculation that depends on energy gap values such as electrofugality ΔE_e and nucleofugality ΔE_n, chemical potential, chemical hardness, electrophilicity index, and electronegativity.

Density functional theory (DFT) B3LYP/6-311G (d,p) calculations were executed for further study on the properties of thermodynamic for the molecule, on the other hand, the parameters of thermodynamic properties like enthalpy, entropy, and heat capacity, were found to be increased with the increasing of the temperature, where the was raised from 200 to 1000 K.

The optimization output of Natural Orbital Occupancy illustrates that the positive charge of the mean ring in the two compounds increased by the presence of benzene ring substitution. The polarizability and hyperpolarizabilities were computed at the same level of theory for all molecules and results indicate that they may possess good nonlinear optical properties.

COMPLIANCE WITH ETHICAL STANDARDS

This article does not contain any studies involving human participants performed by any of the authors and does not contain any studies involving animals performed by any of the authors.

Conflict of Interests

There is no conflict of interest.

REFERENCES

1. Gubler, H.U. and Baggiolini, M., *Scand. J. Rheumatol.*, 1978, vol. 7, no. S21, pp. 8–11. https://doi.org/10.3109/03009747809095666
2. Norton, W.L. and Meisinger, M.A.P., *Inflammation*, 1977, vol. 2, no. 1, pp. 37–46. https://doi.org/10.1007/BF00920873
3. Gerspacher, M., Altmann, E., Beerli, R., Buhl, T., Endres, R., Gamse, R., and Widler, L., *Bioorg. Med. Chem. Lett.*, 2010, vol. 20, no. 17, pp. 5161–5164. https://doi.org/10.1016/j.bmcl.2010.07.016
4. Widler, L., Altmann, E., Beerli, R., Breitenstein, W., Bouhelal, R., Buhl, T., Seuwen, K. *J. Med. Chem.*, 2010, vol. 53, no. 5, pp. 2250–2263. https://doi.org/10.1021/jm901811v

5. Applicationo, B. and Hospital, C., *Biomed. Appl.*, 1985, vol. 341, pp. 106–113. https://doi.org/10.1016/j.bioorg.2016.05.005
6. Raja, M., Muhamed, R. R., Muthu, S., and Suresh, M., *J. Mol. Struct.*, 2017, vol. 1128, pp. 481–492. https://doi.org/10.1016/j.molstruc.2016.09.017
7. Kanungo, B., Zimmerman, P.M., Gavini, V. *Nat. Commun.*, 2019, vol. 10, no. 1, p. 4497. https://doi.org/10.1038/s41467-019-12467-0
8. Electron Density. IUPAC Compendium of Chemical Terminology, 2008, pp. 1–6. https://doi.org/10.1351/goldbook.e01986
9. Bielecki, J. and Lipiec, E., *J. Bioinform. Comp. Biol.*, 2016, vol. 14, no. 1, pp. 1–15. https://doi.org/10.1142/S0219720016500025
10. Sharma, K., Melavanki, R., Patil, S.S., Kusanur, R., Patil, N.R., and Shelar, V.M., *J. Mol. Struct.*, 2019, vol. 1181, pp. 474–487. https://doi.org/10.1016/j.molstruc.2018.12.086
11. Tokay, N., Seferoğlu, Z., Ğretir, C., and Ertan, N., *ARKIVOC*, 2008, vol. 2008, no. 15, pp. 9–20. https://doi.org/10.3998/ark.5550190.0009.f02
12. Kandemirli, F., Saracoglu, M., Amin, M.A., Basaran, M.A., and Vurdu, C.D., *Int. J. Electrochem. Sci.*, 2014, vol. 9, no 7, pp. 3819–3827.
13. Chattaraj, P.K., Sarkar, U., and Roy, D.R., *Chem. Rev.*, 2006, vol. 106, no. 6, pp. 2065–2091. https://doi.org/10.1021/cr040109f
14. Matić, M., Denegri, B., Jurić, S., and Kronja, O., *Croat. Chem. Acta*, 2017, vol. 90, no. 4, pp. 571–581. https://doi.org/10.5562/cca3283
15. Frisch, M.J., Trucks, G.W., Schlegel, H.B., Scuseria, G.E., Robb, M.A., Cheeseman, J.R. and Nakat Suji, H., *Gaussian Inc.*, 2013, pp. 1–20. https://doi.org/10.1159/000348293
16. Dennington, R., Keith, T., and Millam, J., GaussView, Version 5.0.8., Semichem Inc., Shawnee Mission KS, 2009.
17. Lu, T., Plotting electrostatic potential colored molecular surface map with ESP surface extrema via Multiwfn and VMD, 2014.
18. Weinhold, F., Landis, C.R., and Glendening, E.D., *Int. Rev. Phys. Chem.*, 2016, vol. 35, no. 3, pp. 1–42. https://doi.org/10.1080/0144235X.2016.1192262
19. Günay, N., Pir, H., Avci, D., and Atalay, Y., *J. Chem.*, 2013, vol. 2013. https://doi.org/10.1155/2013/712130
20. Reed, A.E., Curtiss, L.A., and Weinhold, F., *Chem. Rev.*, 1988, vol. 88, no. 6, pp. 899–926. https://doi.org/10.1021/cr00088a005
21. Yang, C. and Wang, H., *Struct. Chem.*, 2008, vol. 19, no. 5, pp. 843–847. https://doi.org/10.1007/s11224-008-9374-z
22. Fogolari, F., Corazza, A., and Esposito, G., *Front. Mol. Biosci.*, 2018, vol. 5, pp. 1–5. https://doi.org/10.3389/fmolb.2018.00011
23. Al-Sawaff, Z., Sayiner, H., and Kandemirli, F., *J. Amasya Univ. Ins. Sci. Technol.*, 2020, vol. 1, pp. 1–11. https://dergipark.org.tr/en/pub/jauist/issue/55760/739466.
24. Ford, K.W., *Basic Phys.*, 2017, pp. 371–396. https://doi.org/10.1142/9789813208025_0014
25. Chodera, J.D. and Mobley, D.L., *Annu. Rev. Biophys.*, 2013, vol. 42, no. 1, pp. 121–142. https://doi.org/10.1146/annurev-biophys-083012-130318